

Nature of the first excited state of ${}^4\text{He}$

Attila Csóto* and G. M. Hale†

Theoretical Division, Los Alamos National Laboratory, Los Alamos, New Mexico 87545

(Received 2 January 1997)

We study the first excited state of ${}^4\text{He}$ in a microscopic $\{{}^3\text{H}+p, {}^3\text{He}+n\}$ cluster model, including ${}^3\text{H}$ and ${}^3\text{He}$ distortions. The phenomenological 1S_0 ${}^3\text{H}+p$ scattering phase shift is reasonably well reproduced. We localize a complex pole of the S matrix between the ${}^3\text{H}+p$ and ${}^3\text{He}+n$ thresholds. The corresponding resonance parameters are $E_r=93$ keV position relative to ${}^3\text{H}+p$, and $\Gamma=390$ keV width. A pole search is also performed in an extended R -matrix method, and a resonance is found with parameters $E_r=114$ keV and $\Gamma=392$ keV. The R -matrix approach gives several additional poles, some of which may be connected with an enhanced threshold effect. [S0556-2813(97)03505-X]

PACS number(s): 21.45.+v, 27.10.+h, 21.60.Gx, 25.10.+s

I. INTRODUCTION

${}^4\text{He}$ is the lightest nucleus with a well-established spectrum of excited states. Thus it is an excellent testing ground for nuclear many-body models. Exact four-body calculations with realistic nucleon-nucleon (N - N) interactions have been performed for the 0^+ ground state of ${}^4\text{He}$ by using variational [1] and Green's function Monte Carlo [2] techniques, by solving the Yakubovsky equations [3], and by using the correlated hyperspherical harmonic expansion method [4]. A few excited ${}^4\text{He}$ states have also been studied by a variational Monte Carlo method [5]. However, these latter calculations were performed without the Coulomb interaction, which fact made the theoretical, as well as the Coulomb-corrected experimental 0_2^+ state particle stable. So, the resonant nature of this state could not be studied.

The nuclear shell-model offers another fundamental and, in principle, exact approach to calculate nuclear spectra. Early shell-model calculations, restricted to $(0+1)\hbar\omega$ excitations, failed to provide a satisfactory description of both the ground-state properties and the excitation spectrum of ${}^4\text{He}$ [6]. It was realized that higher $\hbar\omega$ excitations play important roles in ${}^4\text{He}$, especially in the excited states [7]. The shell-model calculations were substantially improved by using a $10\hbar\omega$ model space with various N - N interactions [8]. Those authors extensively studied the question of whether the ground (0_1^+) and first excited (0_2^+) states can be described simultaneously in a consistent way. It turned out that using a harmonic-oscillator-size parameter that is optimal for the ground state in the calculations for the 0_2^+ excited state made the excitation energy either several MeV too large or too small depending on the N - N interaction. The usual resonance prescription puts this 0_2^+ first excited state between the ${}^3\text{H}+p$ and ${}^3\text{He}+n$ thresholds at $E_r=395$ keV (all energies are given in this paper in the center-of-mass frame, relative to the ${}^3\text{H}+p$ threshold) [9]; thus, delicate effects of few-body dynamics are expected to play an important role. The 0_2^+ state is generally viewed as a one-particle-one-hole

“breathing” excitation of the ground state. In Ref. [8] it was found that the charge radius of the 0_2^+ state is significantly larger than that of the 0_1^+ ground state, while the D -state probabilities are similar. The authors interpreted these findings as support for the breathing-mode interpretation.

Recently a series of calculations have been performed for ${}^4\text{He}$ and for other light nuclei in large, no-core shell models, using interactions derived from realistic N - N forces [10]. The model reproduced the experimental ${}^4\text{He}$ spectrum rather well, except for the 0_2^+ state [10]. This state was not the first excited state in that model as its excitation energy exceeded the experimental one by more than 10 MeV in a $4\hbar\omega$ shell-model space. In larger model spaces the 0_2^+ state gradually moved toward lower energies, and in a $8\hbar\omega$ calculation it was found to be the second excited state, some 1.5 MeV higher in energy than experimentally [11]. Its position relative to the $3+1$ thresholds could not be determined because the starting-energy dependence of the model made comparisons between the energies of different nuclei rather ambiguous. Recently the starting-energy dependence was removed from that model, thus allowing excited states to be referenced to breakup thresholds [12]. The 0_2^+ state was found to be the second excited state situated above the ${}^3\text{He}+n$ threshold of that model [12]. Thus, its shell-model description still needs improvements.

We would like to emphasize here that shell-model calculations use unphysical boundary conditions for scattering wave functions [13]. It means that by increasing the shell-model space, the energy of an unbound state converges not to the resonance energy, but to the lowest two-body threshold [13], or to ${}^3\text{H}+p$ in the present case. In such a case, the shell-model wave function describes a situation where three nucleons stay close to each other forming a triton, while the fourth nucleon (proton) is far away.

The shell-model wave function mimics a scattering wave function that has a node at the spatial range of the last shell-model basis function. If the phase shift in the two-body channel shows a sharp increase at a given energy, which is a sign of a resonance, then the shell-model energy is almost stable with respect to large variations of the spatial range of the basis, i.e., the size of the shell-model space. This means that the shell-model energy has as a function of the size of the

*Electronic address: csoto@qmc.lanl.gov

†Electronic address: gmh@t2.lanl.gov

model space a plateau, from which, in principle, the position and width of the resonance can be extracted [14].

The origin of the great difficulties of the shell model to reproduce the 0_2^+ state at the correct excitation energy, between the ${}^3\text{H}+p$ and ${}^3\text{He}+n$ thresholds, is obvious. The closeness of this state to those two-body channels means that the most relevant degrees of freedom are the ${}^3\text{H}+p$ and ${}^3\text{He}+n$ relative motions. Thus, configurations that describe the ${}^3\text{H}+p$ and ${}^3\text{He}+n$ clustering have large weight in the wave function. It is known that wave functions which explicitly contain two-body (or three-body) clustering, correspond to shell-model states with very high $\hbar\omega$ excitations [15]. The shell model treats all degrees of freedom equally, so it requires very large model spaces to correctly reproduce the two-cluster correlations.

In the present work we study the 0_2^+ state of ${}^4\text{He}$ in a microscopic cluster model. Contrary to the shell-model, this approach emphasizes the two-cluster correlations by building up the wave function from configurations with two-body dynamical degrees of freedom. Recently the spectrum of ${}^4\text{He}$ has been extensively studied in a cluster model [16]. We do not repeat here all those calculations. Our prime target is the 0_2^+ state, and we also study the 0_1^+ ground state. The nature of the 0_2^+ state is not well understood. For example, in [9] it was speculated that this state might originate from an S -matrix pole far away from the physical region, and several MeV higher in energy than its 395 keV experimental excitation energy would suggest. In the present work we study the problem at complex energies, and try to reveal the pole structure of the S matrix. The same method has recently been used to study the $3/2^-$ and $1/2^-$ low-lying states of ${}^5\text{He}$ and ${}^5\text{Li}$ [17]. Some further details can be found there.

II. RESONATING GROUP MODEL (RGM)

We use a microscopic two-cluster resonating group model (RGM) approach to ${}^4\text{He}$. The trial function of the four-body system is

$$\begin{aligned} \Psi = & \sum_{i=1}^{N_t} \sum_{S,L} \mathcal{A}\{[(\Phi^{t_i}\Phi^p)]_S \chi_L^{t_i p}(\boldsymbol{\rho}_{tp})\}_{JM} \\ & + \sum_{i=1}^{N_h} \sum_{S,L} \mathcal{A}\{[(\Phi^{h_i}\Phi^n)]_S \chi_L^{h_i n}(\boldsymbol{\rho}_{hn})\}_{JM} \\ & + \sum_{i,j=1}^{N_d} \sum_{S,L} \mathcal{A}\{[(\Phi^{d_i}\Phi^{d_j})]_S \chi_L^{d_i d_j}(\boldsymbol{\rho}_{dd})\}_{JM}, \quad (1) \end{aligned}$$

where \mathcal{A} is the intercluster antisymmetrizer, the $\boldsymbol{\rho}$ vectors are the various intercluster Jacobi coordinates, L and S is the total angular momentum and spin, respectively, and $[\dots]$ denotes angular momentum coupling. While Φ^p and Φ^n is a neutron and proton spin-isospin eigenstate, respectively, the antisymmetrized ground state ($i=1$) and continuum excited distortion states ($i>1$) of the t , h , and d clusters ($t={}^3\text{H}$, $h={}^3\text{He}$, and $d={}^2\text{H}$) are represented by the wave functions

$$\begin{aligned} \Phi^{t_i} &= \sum_{j=1}^{N_t} A_{ij}^t \phi_{\beta_j}^t, \quad i=1,2,\dots,N_t, \\ \Phi^{h_i} &= \sum_{j=1}^{N_h} A_{ij}^h \phi_{\beta_j}^h, \quad i=1,2,\dots,N_h, \\ \Phi^{d_i} &= \sum_{j=1}^{N_d} A_{ij}^d \phi_{\beta_j}^d, \quad i=1,2,\dots,N_d. \quad (2) \end{aligned}$$

Here $\phi_{\beta_j}^t$, $\phi_{\beta_j}^h$, and $\phi_{\beta_j}^d$ are translationally invariant $0s$ harmonic-oscillator shell-model wave functions of t , h , and d , respectively, with size parameter β_j , and the A_{ij} parameters are to be determined by minimizing the energies of the free clusters [18]. Our choice of L , S , N_t , N_h , and N_d will be discussed later. Putting Eq. (1) into the four-nucleon Schrödinger equation which contains a two-nucleon strong and Coulomb interaction, we get an equation for the inter-cluster relative motion functions χ . For bound states, these relative motion functions are expanded in terms of square-integrable tempered Gaussian functions [19], and the expansion coefficients are determined from a variational method. For scattering states, we employ a Kohn-Hulthén variational method for the S matrix, which uses square-integrable basis functions matched with the correct scattering asymptotics [19].

III. RESULTS AND DISCUSSION

A. RGM

For the N - N force we use the Minnesota (MN) effective interaction [20] together with the tensor force of [21]. The MN interaction reproduces the deuteron binding energy in a 3S_1 model space without the D state, which means that the interaction is too strong in the 3S_1 partial wave [22]. For the ground and first excited $J^\pi=0^+$ states we use $L=S=0$ in the ${}^3\text{H}+p$ and ${}^3\text{He}+n$ configurations, and $L=S=0$ and $L=S=2$ in the $d+d$ configurations (the deuteron spin is 1). The $d+d$ configurations contain 3S_1 N - N states, so we can expect that a model space which contains these configurations leads to unphysical overbinding. We use four different model spaces: (i) $N_t=N_h=1$ and there is no $d+d$ component; (ii) $N_t=N_h=3$ and there is no $d+d$ component; (iii) $N_t=N_h=3$, $N_d=1$ and only the $L=S=0$ state is present in the $d+d$ channel; (iv) $N_t=N_h=3$, $N_d=1$ and both the $L=S=0$ and $L=S=2$ states are present in the $d+d$ channel. The $E_{tp}-E_{hn}$ threshold energy difference is 0.768 and 0.745 MeV for the $N_t=N_h=1$ and $N_t=N_h=3$ model spaces, respectively. It is to be compared to the 0.763 MeV experimental value. Our $d+d$ threshold is 6.8 MeV above the ${}^3\text{H}+p$ one in the $N_t=N_h=3$ model, while the experimental value is 4.0 MeV.

Due to the 3S_1 overbinding problem, model spaces (iii) and (iv) are rather unphysical. We use them only for test purposes; that is why we do not allow for distortions in the deuteron clusters in Eq. (2). We note, that Ref. [16] used an N - N interaction which was free from the above defect, so the model worked in a full $\{{}^3\text{He}+p, {}^3\text{He}+n, d+d\}$ space without any problem. Our main purpose is to localize the 0_2^+ state. Test calculations for other systems, for instance for the

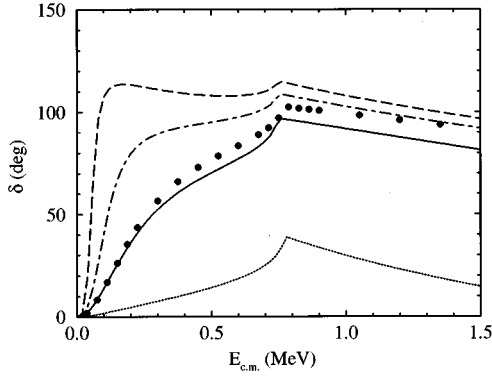


FIG. 1. 1S_0 phase shifts for $^3\text{H}+p$ scattering, coming from model spaces (i)—dotted line, (ii)—solid line, (iii)—dash-dotted line, and (iv)—dashed line. Model spaces (i)–(iv) are defined in the text. The solid dots come from an R -matrix analysis of the experimental data [16].

$3/2^+$ state of ^5He [23,24], show that in order to reproduce experimental resonance parameters, one really needs to reproduce only the relevant experimental phase shifts. This is true even if the description of the free clusters is highly unphysical, e.g., if they are unbound [24].

The most relevant phase shift in the present problem is that for 1S_0 $^3\text{H}+p$. In Fig. 1 we show this phase shift coming from the various model spaces. We note that both the phase shifts and the binding energies are almost totally insensitive to the mixing parameter u of the N - N interaction. We use $u=0.98$ and the corresponding variationally stabilized oscillator size parameters for the clusters. One can see in Fig. 1 that the effect of the ^3H and ^3He distortions is significant, and that the model spaces which contain $d+d$ components show the overbinding effect, as expected. Thus, our best model is model (ii) with $N_t=N_h=3$ and without the $d+d$ configurations.

First we perform calculations for $J^\pi=0^+$ states by applying bound state asymptotics in Eq. (1). This wave function satisfies the correct physical asymptotics only for states

which are below all the breakup thresholds, i.e., below the $^3\text{H}+p$ threshold in the present problem. For states above this threshold, this is a bound state approximation, like in the shell-model. In Table I we show the positions of the two lowest 0^+ states in the various model spaces together with the amounts of clustering of the various configurations. This latter quantity gives the probability that the wave function is entirely in the given subspace [25,26]. Thus it is a useful measure of the relative importance of nonorthogonal channels.

The 0_1^+ ground state is slightly overbound compared to the $E_r = -19.815$ MeV experimental value [9]. Each model space predicts the 0_2^+ state between the $^3\text{H}+p$ and $^3\text{He}+n$ thresholds. One can see from the amounts of clustering of the various configurations, that in the ground state the $^3\text{H}+p$ and $^3\text{He}+n$ clusterizations are equally important, while 0_2^+ is predominantly a $^3\text{H}+p$ state. The small amount of $(L,S)=(2,2)$ $d+d$ clustering in Table I shows that the inclusion of the $d+d$ channel, and thus the D state, is rather schematic in our model, because of the $0s$ nature of our deuteron. We mention that the role of the tensor force and that of the D state in the ground state of ^4He was thoroughly studied, e.g., in [27]. The results of those works show that the full inclusion of the $d+d$ channel (with D states in the deuterons) would be a major improvement in our model, especially in the 0_1^+ ground state.

The point nucleon rms radius of the ground state is around 1.6 fm in our model, only slightly larger than the 1.48 fm experimental value. However, the radius corresponding to the 0_2^+ state is huge, being around 40 fm. This is an unphysical value, which shows that the bound state approximation to a state which is above breakup thresholds might not make much sense [13]. So, the conclusions of Ref. [8] concerning the breathing mode are questionable.

For a reliable localization of a state above breakup thresholds, the correct scattering asymptotics in the various channels must be imposed. Then one can search for resonant states either by studying the phase shifts, or by exploring the

TABLE I. Energies (relative to $^3\text{H}+p$) of the 0_1^+ and 0_2^+ states of ^4He , and the amounts of clustering of the various cluster configurations in these states in model spaces (i)–(iv), defined in the text. The three numbers in parentheses are for the three ^3H or ^3He states, in the case of $N_t=3$ or $N_h=3$. In the $d+d$ channels the (L,S) values are also given.

Model	0_1^+			0_2^+		
	E (MeV)	Amount of clustering		E (MeV)	Amount of clustering	
(i)	-20.83	$^3\text{H}+p$	97.5	0.54	$^3\text{H}+p$	90.0
		$^3\text{He}+n$	97.3		$^3\text{He}+n$	11.9
(ii)	-20.53	$^3\text{H}+p$	(94.8,10.5,0.05)	0.34	$^3\text{H}+p$	(80.4,16.5,0.07)
		$^3\text{He}+n$	(94.5,11.5,0.05)		$^3\text{He}+n$	(27.8,19.7,0.08)
(iii)	-20.66	$^3\text{H}+p$	(94.6,10.5,0.04)	0.24	$^3\text{H}+p$	(76.2,20.0,0.08)
		$^3\text{He}+n$	(94.2,11.5,0.05)		$^3\text{He}+n$	(32.6,23.3,0.09)
(iv)	-21.63	$d+d$ (0,0)	59.5	0.15	$d+d$ (0,0)	27.2
		$^3\text{H}+p$	(93.1,10.7,0.04)		$^3\text{H}+p$	(73.8,22.9,0.09)
		$^3\text{He}+n$	(92.7,11.7,0.04)		$^3\text{He}+n$	(36.1,26.2,0.09)
		$d+d$ (0,0)	58.3		$d+d$ (0,0)	30.4
		$d+d$ (2,2)	1.4		$d+d$ (2,2)	0.3

pole structure of the scattering matrix. In order to avoid any ambiguity in the recognition of a resonance in the phase shift, we choose here the latter method. We solve the Schrödinger equation for the relative motion functions χ in Eq. (1) at complex energies with the following boundary conditions for $\rho \rightarrow \infty$

$$\chi_L^{ab}(\varepsilon, \rho_{ab}) \rightarrow H_L^-(k\rho_{ab}) - S_L(\varepsilon)H_L^+(k\rho_{ab}). \quad (3)$$

Here ε and k are the *complex* energies and wave numbers of the relative motions between clusters a and b , and H^- and H^+ are the incoming and outgoing Coulomb functions, respectively. We search for the poles of S by extending the coupled channel scattering approach of Ref. [19] to complex energies [23,17]. The complex Coulomb functions are calculated by using Ref. [28]. The resulting complex energies ε of the poles are connected to the resonance parameters via

$$\varepsilon = E_r - i\Gamma/2, \quad (4)$$

where E_r is the position of the resonance, and Γ is its width.

In the case of an N -channel scattering problem, the complex channel wave numbers k_1, k_2, \dots, k_N , which determine the character of a state (bound state, scattering state, resonance) can be mapped by a one-to-one mapping to the 2^N -sheeted Riemann surface of the complex channel energies $\varepsilon_1, \varepsilon_2, \dots, \varepsilon_N$ [29]. The sheets of this surface can be labeled by an N -term sign string given by the signs of the imaginary parts of the channel wave numbers $[\text{sgn}(\text{Im}k_1), \text{sgn}(\text{Im}k_2), \dots, (\text{Im}k_N)]$. It has been shown [29,30] that in the case of Hermitian potentials, a complex pole of the S matrix that would appear in one of the N channels in a single-channel problem, gives rise to 2^{N-1} poles on different Riemann sheets in the N -channel problem. The proof of this statement is based on the fact that in the zero-coupling limit, when the only coupling is the energy conservation, the $N \times N$ Fredholm determinant of an N -channel scattering problem reduces to the product of N one-channel Fredholm determinants. However, the situation is different if there are nonorthogonal channels, like the $(L,S)=(0,0)$ ones in the present case. Such channels are inherently coupled, and the zero-coupling limit cannot be taken. In such cases one does not know the number and location of the poles, so one has to search all energy sheets.

Following [29], the poles lying on the sheet closest to the physical sheet ($[++++]$) at a given energy, are called conventional poles, while the others are called shadow poles. Usually only the conventional poles have observable effects, causing the appearance of conventional resonances. However, there are exceptions where the effects of shadow poles are non-negligible or even dominant. We mention here the examples of the ${}^3\text{H}(d,n){}^4\text{He}$ reaction [31,23] and the structure of ${}^8\text{Be}$ [32]. Shadow poles play an important role also in atomic physics, in laser ionization processes, because of the large number of channels and relatively low energies required for ionization [33]. In Ref. [9] it was speculated that the 0_2^+ state of ${}^4\text{He}$ might come from a shadow pole, which fact could partly explain the difficulties encountered by the shell model in reproducing this state at the correct energy.

In order to explore this possibility, we searched all energy sheets for poles. In model spaces that include ${}^3\text{H}$ and ${}^3\text{He}$

distortions, the continuum excited distortion states represent high-lying channels, e.g., in model space (ii) we have six channels: $\{t_1+p, t_2+p, t_3+p, h_1+n, h_2+n, h_3+n\}$. The dominant Riemann sheets are those where the distortion channels all have bound state character (+), rather than antibound state character (-). In the case of model (ii) these dominant sheets are $[++++]$, $[+++ - ++]$, $[- + + + +]$, and $[- + + - + +]$. Numerical studies show [24] that if there is an S -matrix pole on one of these sheets, then the corresponding pole on a sheet, where the character of at least one distortion channel is “-,” is situated almost exactly at the same complex energy position as the original pole. Since these latter sheets are much farther from the physical region than the four dominant ones, their poles have negligible observable effect. That is why we set the character of all distortion channels to “+” and give only the characters of those channels that contain the ground states of the clusters; e.g., $[- -]$ means $[- + + - + +]$ in model space (ii).

In model space (i) we do not find any pole, while in the (ii), (iii), and (iv) model spaces we find one pole on the $[- +]$, $[- + +]$, and $[- + +]$ sheets, respectively at $(0.093 - i0.195)$, $(0.085 - i0.071)$, and $(0.053 - i0.021)$ MeV complex energies, respectively. (Note that the thresholds of the two $d+d$ channels coincide, so the character of the fourth channel is always the same as that of the third one.) One can see the effect of the 3S_1 overbinding problem in the pole positions in the (iii) and (iv) models. In each model space the pole is on the Riemann sheet which is closest to the physical sheet, i.e., it is a conventional pole. We do not find any other pole on any other sheet in the vicinity of the ${}^3\text{H}+p$ and ${}^3\text{He}+n$ channel thresholds.

To recap the results of the RGM calculations, our best model with ${}^3\text{H}$ and ${}^3\text{He}$ distortions predicts the 0_2^+ state to be a conventional resonance at $E_r=93$ keV above the ${}^3\text{H}+p$ threshold, with 390 keV width.

B. R -matrix

The RGM results encouraged us to search again for this state as an S -matrix pole in the charge-independent R -matrix analysis of reactions in the $A=4$ system reported in Refs. [9] and [16]. The state was visible at $E=395$ keV according to the usual resonance-parameter prescription, but did not appear to give a low-lying S -matrix pole using the “extended” R -matrix prescription [31,17]. This prescription involves first fitting the available experimental data in terms of the conventional R -matrix parametrization at real energies on the physical sheet, then using this parametrization to continue the S matrix onto other sheets of the Riemann energy surface in order to study its analytic structure [31], in very much the same way as discussed above.

The channel configuration and the distribution by reaction of data included in the $A=4$ R -matrix analysis are summarized in Table II, taken from Ref. [16]. In general, all types of cross-section and polarization measurements were used, but the ones that showed most clearly the 0^+ resonance and its associated threshold effect were excitation functions of the ${}^3\text{H}(p,p){}^3\text{H}$ differential elastic cross section [34–38]. Some of those measurements are shown compared with the R -matrix calculation in Fig. 2. The resonance peak occurs at

TABLE II. Channel configuration (top) and data summary (bottom) for each reaction in the ${}^4\text{He}$ system R -matrix analysis. The maximum orbital angular momentum allowed for each arrangement is given by l_{\max} , while a_c is the channel radius.

Channel	l_{\max}	a_c (fm)
${}^3\text{H}+p$	3	4.9
${}^3\text{He}+n$	3	4.9
$d+d$	3	7.0

Reaction	Energy range (MeV)	No. observable types	No. data points
${}^3\text{H}(p,p){}^3\text{H}$	$E_p=0-11$	3	1382
${}^3\text{H}(p,n){}^3\text{He} + {}^3\text{He}(n,p){}^3\text{H}$	$E_p=0-11$	5	726
${}^3\text{He}(n,n){}^3\text{He}$	$E_n=0-10$	2	126
${}^2\text{H}(d,p){}^3\text{H}$	$E_d=0-10$	6	1382
${}^2\text{H}(d,n){}^3\text{He}$	$E_d=0-10$	6	700
${}^2\text{H}(d,d){}^2\text{H}$	$E_d=0-10$	6	336
Totals:		28	4652

about 350 keV, and the threshold step at $E=764$ keV is especially striking at this angle ($\theta_{\text{c.m.}}=120^\circ$). The resulting 1S_0 ${}^3\text{H}+p$ phase shift, represented by the dots in Fig. 1, serves as the ‘‘experimental’’ data to which the RGM results are compared.

We find an S -matrix pole on the $[-++]$ sheet at $(0.114-i0.196)$ MeV, corresponding to a conventional resonance at $E_r=114$ keV above the ${}^3\text{H}+p$ threshold, with $\Gamma=392$ keV width, in good agreement with the parameters obtained from the RGM. At the time of the ${}^4\text{He}$ level compilation reported in [9], this pole had not been found because the step size of the automated search algorithm was too large, leading to the speculation that the resonance might actually be associated with higher-lying shadow poles in the 0^+ state. These shadow poles occur at energies between about 3.0 and 3.6 MeV, with widths in the range 6–8 MeV, on the Riemann sheets $[-++]$, $[-+-]$, $[+-]$, and $[+ - +]$. In addition, there is another resonance at $\varepsilon=(7.68-i3.57)$ MeV on the $[- - -]$ sheet, with an associated shadow pole at $\varepsilon=(8.43-i3.43)$ MeV on the $[- - +]$ sheet.

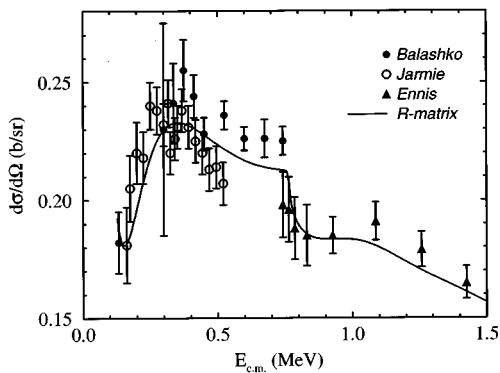


FIG. 2. Differential cross section for ${}^3\text{H}(p,p){}^3\text{H}$ elastic scattering at $\theta_{\text{c.m.}}\approx 120^\circ$. The solid curve is the R -matrix calculation, and the data are from Refs. [34,35] (solid circles), [37] (open circles), and [38] (solid triangles).

It is interesting to note that all of the S -matrix structure described above comes predominantly from the same $T=0$ level in the R matrix, located approximately 6 MeV above the ${}^3\text{H}+p$ threshold. The position of this level depends on the boundary conditions, which are taken to be the shift functions in the various channels¹ evaluated at the ground-state energy of ${}^4\text{He}$, so that the lowest 0^+ R -matrix level coincides identically with the ${}^4\text{He}$ ground state. One can then imagine the 6-MeV level to be associated with a small-basis shell-model wave function, since these states, like the internal R -matrix eigenfunctions, are expected to represent the true wave function of the scattering system only in a limited region of space. The point is that, when such an expansion is matched to the correct asymptotic scattering solution, it produces a low-lying S -matrix pole in the correct position for the resonance associated with the first excited state of ${}^4\text{He}$, even though the energy eigenvalue of the structure state is far above the resonance energy. Of course, as was discussed earlier, enlarging the shell-model basis would make the energy of the state decrease until, at some point, it would pass through the resonance energy on the way to attaining its minimum value (the ${}^3\text{H}+p$ threshold energy). However, the correct information about the resonance as an S -matrix pole may already be contained in the small-basis shell-model states.

As was noted earlier, the additional poles above the ${}^3\text{He}+n$ threshold were not found in the RGM approach. Compared to the R -matrix model, our RGM approach is less realistic, mainly because the description of the $d+d$ channels is rather schematic due to the 3S_1 force problem. On the other hand, the R -matrix approach embodies some aspects of channel orthogonality in the region outside the nuclear surface that might increase the likelihood of having multiple poles (cf. the discussion about the number of poles in an

¹The boundary condition used in the 3+1 channels is actually the average of the ${}^3\text{H}+p$ and ${}^3\text{He}+n$ shifts, in order to preserve the charge-independent model.

N -channel scattering problem). The nature of these additional states in the R -matrix spectrum will require further investigation. However, they appear to be necessary in order to enhance the strong threshold step that is seen in the measured ${}^3\text{H}+p$ cross-section excitation functions.

Both calculations are in substantial agreement that the first excited state of ${}^4\text{He}$ is 0_2^+ , a conventional resonance lying between the ${}^3\text{H}+p$ and ${}^3\text{He}+n$ thresholds, with $E_r \approx 100$ keV energy relative to ${}^3\text{H}+p$, and $\Gamma \approx 400$ keV. Since the real-energy resonance parameters for this state, $E_r = 395$ keV and $\Gamma = 500$ keV [9], were obtained from the same R -matrix parameters as used here, the differences come entirely from the relation of resonance parameters determined from real- and complex-energy scattering quantities, respectively, as discussed in Ref. [17].

IV. CONCLUSION

In summary, we have described the 0_1^+ and 0_2^+ states of ${}^4\text{He}$ in a microscopic $\{{}^3\text{H}+p, {}^3\text{He}+n\}$ RGM approach. The effective interaction did not allow us to fully include $d+d$ configurations into the model. We have found that ${}^3\text{H}$ and ${}^3\text{He}$ cluster distortions play important roles if one wants to reproduce the relevant 1S_0 ${}^3\text{H}+p$ phase shift. Our best model, which satisfactorily reproduced this phase shift, put the ground state of ${}^4\text{He}$ at -20.53 MeV relative to the

${}^3\text{H}+p$ threshold. We have searched for S -matrix poles at complex energies using the same model space, and found one at $(0.093 - i0.195)$ MeV energy, relative to the ${}^3\text{H}+p$ threshold. Our model predicts that this 0_2^+ state is the first excited state of ${}^4\text{He}$, and is a conventional resonance at $E_r = 93$ keV with $\Gamma = 390$ keV width. While in the ground state both the ${}^3\text{H}+p$ and the ${}^3\text{He}+n$ configurations have roughly the same weight, the 0_2^+ state is dominated by the ${}^3\text{H}+p$ configuration.

We have also localized the 0_2^+ state in an extended R -matrix model. Its parameters $E_r = 114$ keV and $\Gamma = 392$ keV are in good agreement with the RGM parameters. The R -matrix model produces several additional 0^+ poles. While the understanding of these structures will require further theoretical investigation, their role in producing a strong threshold effect is already clearly seen.

ACKNOWLEDGMENTS

This work was performed under the auspices of the U.S. Department of Energy. Early stages of this work were done at the National Superconducting Cyclotron Laboratory at Michigan State University, supported by NSF Grant Nos. PHY92-53505 and PHY94-03666. Support from OTKA Grant No. F019701 is also acknowledged.

-
- [1] J. Carlson, V. R. Pandharipande, and R. B. Wiringa, Nucl. Phys. **A401**, 59 (1983); R. B. Wiringa, Phys. Rev. C **43**, 1585 (1991).
- [2] J. Carlson, Phys. Rev. C **38**, 1879 (1988); B. S. Pudliner, V. R. Pandharipande, J. Carlson, and R. B. Wiringa, Phys. Rev. Lett. **74**, 4396 (1995).
- [3] W. Glöckle and H. Kamada, Phys. Rev. Lett. **71**, 971 (1993).
- [4] M. Viviani, A. Kievsky, and S. Rosati, Few-Body Syst. **18**, 25 (1995).
- [5] J. Carlson, V. R. Pandharipande, and R. B. Wiringa, Nucl. Phys. **A424**, 47 (1984).
- [6] A. de Shalit and J. D. Walecka, Phys. Rev. **147**, 763 (1966); B. R. Barrett, *ibid.* **154**, 955 (1967); T. T. S. Kuo and J. B. McGrory, Nucl. Phys. **A134**, 633 (1969); P. P. Szydlik, J. R. Borysowicz, and R. F. Wagner, Phys. Rev. C **6**, 1902 (1972); P. P. Szydlik, *ibid.* **1**, 146 (1970); A. G. M. van Hees and P. W. M. Glaudemans, Z. Phys. A **315**, 223 (1984).
- [7] J. J. Bevelacqua and R. J. Philpott, Nucl. Phys. **A275**, 301 (1977); J. J. Bevelacqua, Can. J. Phys. **57**, 1833 (1979).
- [8] R. Ceuleneer, P. Vandeputte, and C. Semay, Phys. Rev. C **38**, 2335 (1988); see also R. Ceuleneer, P. Vandeputte, and C. Semay, Phys. Lett. B **196**, 303 (1987); R. Ceuleneer and P. Vandeputte, Phys. Rev. C **31**, 1528 (1985).
- [9] D. R. Tilley, H. R. Weller, and G. M. Hale, Nucl. Phys. **A541**, 1 (1992).
- [10] D. C. Zheng, B. R. Barrett, L. Jaqua, J. P. Vary, and R. J. McCarthy, Phys. Rev. C **48**, 1083 (1993).
- [11] D. C. Zheng, J. P. Vary, and B. R. Barrett, Phys. Rev. C **50**, 2841 (1994); D. C. Zheng, B. R. Barrett, J. P. Vary, W. C. Haxton, and C. L. Song, *ibid.* **52**, 2488 (1995).
- [12] P. Navrátil and B. R. Barrett, Phys. Rev. C **54**, 2986 (1996).
- [13] A. Csóto and R. G. Lovas, Phys. Rev. C **53**, 1444 (1996).
- [14] A. U. Hazi and H. S. Taylor, Phys. Rev. A **1**, 1109 (1970).
- [15] Y. Suzuki, K. Arai, Y. Ogawa, and K. Varga, Phys. Rev. C **54**, 2073 (1996).
- [16] H. M. Hofmann and G. M. Hale, Nucl. Phys. **A613**, 69 (1997).
- [17] A. Csóto and G. M. Hale, Phys. Rev. C **55**, 536 (1997).
- [18] P. N. Shen, Y. C. Tang, Y. Fujiwara, and H. Kanada, Phys. Rev. C **31**, 2001 (1985).
- [19] M. Kamimura, Prog. Theor. Phys. Suppl. **62**, 236 (1977).
- [20] D. R. Thompson, M. LeMere, and Y. C. Tang, Nucl. Phys. **A268**, 53 (1977); I. Reichstein and Y. C. Tang, *ibid.* **A158**, 529 (1970); see also Ref. [26].
- [21] P. Heiss and H. H. Hackenbroich, Phys. Lett. **30B**, 373 (1969).
- [22] A. Csóto and D. Baye, Phys. Rev. C **49**, 818 (1994); A. Csóto, *ibid.* **49**, 3035 (1994).
- [23] A. Csóto, R. G. Lovas, and A. T. Kruppa, Phys. Rev. Lett. **70**, 1389 (1993).
- [24] A. Csóto, Ph.D. Thesis, Kossuth University, 1992.
- [25] R. Beck, F. Dickmann, and R. G. Lovas, Ann. Phys. (N.Y.) **173**, 1 (1987).
- [26] A. Csóto, Phys. Rev. C **48**, 165 (1993).
- [27] A. C. Fonseca, Phys. Rev. C **40**, 1390 (1989); A. C. Fonseca, B. F. Gibson, and D. R. Lehman, *ibid.* **48**, 2528 (1993).
- [28] I. J. Thompson and A. R. Barnett, Comput. Phys. Commun. **36**, 363 (1985); J. Comput. Phys. **64**, 490 (1986).
- [29] R. J. Eden and J. R. Taylor, Phys. Rev. **133**, B1575 (1964).
- [30] B. C. Pearce and B. F. Gibson, Phys. Rev. C **40**, 902 (1989).
- [31] G. M. Hale, R. E. Brown, and N. Jarmie, Phys. Rev. Lett. **59**, 763 (1987).

- [32] P. E. Koehler *et al.*, Phys. Rev. C **37**, 917 (1988).
- [33] R. M. Potvliege and R. Shakeshaft, Phys. Rev. A **38**, 6190 (1988); M. Dörr and R. M. Potvliege, *ibid.* **41**, 1472 (1990).
- [34] Yu. G. Balashko, I. Ya. Barit, and Y. A. Goncharov, Zh. Eksp. Teor. Fiz. **36**, 1937 (1959) [Sov. Phys. JETP **9**, 1378 (1959)].
- [35] Yu. G. Balashko, I. Ya. Barit, L. S. Dul'kova, and A. B. Kurepin, Zh. Eksp. Teor. Fiz. **46**, 1903 (1964) [Sov. Phys. JETP **19**, 1281 (1964)].
- [36] N. Jarmie and R. C. Allen, Phys. Rev. **114**, 176 (1959).
- [37] N. Jarmie, M. G. Silbert, D. B. Smith, and J. S. Loos, Phys. Rev. **130**, 1987 (1963).
- [38] M. E. Ennis and A. Hemmendinger, Phys. Rev. **95**, 772 (1954).